

**UCSF**

**UC San Francisco Electronic Theses and Dissertations**

**Title**

Improved chemoenzymatic radiosynthesis of fluorine-18 labeled sakebiose for microPET-CT imaging of Staphylococcus aureus

**Permalink**

<https://escholarship.org/uc/item/1qs6r2sd>

**Author**

Urmanov, Nadezhda A.

**Publication Date**

2024

Peer reviewed|Thesis/dissertation

Improved chemoenzymatic radiosynthesis of fluorine-18 labeled sakebiose for  
microPET-CT imaging of Staphylococcus aureus

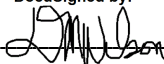
by  
Nadezhda A. Urmanov

THESIS  
Submitted in partial satisfaction of the requirements for degree of  
MASTER OF SCIENCE

in  
Biomedical Imaging

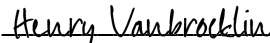
in the  
GRADUATE DIVISION  
of the  
UNIVERSITY OF CALIFORNIA, SAN FRANCISCO

Approved:

DocuSigned by:  
  
A6A8271DA18044C... David M Wilson  
Chair

DocuSigned by:  
  
484... seo, youngho

DocuSigned by:  
  
484... Michael Evans

DocuSigned by:  
  
45037357DDBB24B1... Henry Vanbrocklin

---

Committee Members



## **ACKNOWLEDGEMENT**

I would like to thank Marina Lopez-Alvarez, Ph.D.; Wenxing, Zou Ph.D.; Junaid Ur Rahim, Ph.D.; Sang Hee Lee, Ph.D.; Michael Evans, Ph.D.; Seo Youngho, Ph.D.; Henry VanBrocklin, Ph.D.; David M. Wilson, Ph.D./M.D.; for their valuable insights into designing the experiment and for their helpful discussions.

Improved chemoenzymatic radiosynthesis of fluorine-18 labeled sakebiose for microPET-CT imaging of  
*Staphylococcus aureus*.

Nadezhda A. Urmanov

#### Abstract

*Staphylococcus aureus* (*S. aureus*) is a gram-positive bacterium that can cause severe infections such as pneumonia, osteomyelitis, and endocarditis when it breaches the skin. This study aimed to enhance the chemoenzymatic radiosynthesis of 2-deoxy-2-[<sup>18</sup>F]-fluoro-sakebiose ([<sup>18</sup>F]FSK), a radiotracer potentially useful for imaging *S. aureus* infections. By optimizing the synthesis of 2-deoxy-2-[<sup>19</sup>F]-fluoro-sakebiose ([<sup>19</sup>F]FSK), we identified key factors—such as increased enzyme concentration and decreased precursor levels—that significantly improved the yield. Applying these optimized conditions to the synthesis of [<sup>18</sup>F]FSK resulted in a 30% increase in the radiochemical yield (RCY%) from the control experiment. *In vitro* evaluation showed that [<sup>18</sup>F]FSK was successfully incorporated into two strains of *S. aureus*, suggesting its potential utility for imaging bacterial infections *in vivo*. This work lays the groundwork for using [<sup>18</sup>F]FSK in PET/CT imaging to diagnose and monitor *S. aureus* infections.

## TABLE OF CONTENTS

Abstract .....	3
Introduction .....	9
Goals .....	10
Methods .....	10
Materials .....	10
Preparation of beta-D-glucose-1-phosphate .....	11
[ <sup>19</sup> F]FSK Synthesis .....	11
[ <sup>19</sup> F]FSK NMR Preparation .....	11
[ <sup>18</sup> F]FSK Synthesis .....	11
<i>In vitro</i> Uptake Evaluation in <i>Staphylococcus aureus</i> .....	12
μPET/CT imaging .....	13
Results .....	13
Beta-D-glucose-1-phosphate .....	13
[ <sup>19</sup> F]FSK Trials .....	14
[ <sup>18</sup> F]FSK Trials .....	17
[ <sup>18</sup> F]FSK <i>In vitro</i> Uptake Evaluation in <i>Staphylococcus aureus</i> .....	22
[ <sup>18</sup> F]FSK <i>In Vivo</i> Dynamic Imaging .....	22
Discussion .....	23
Conclusion .....	25
Reference .....	26

## LIST OF TABLES

<b>Table 1.</b> [ $^{19}\text{F}$ ]FSK chemoenzymatic synthesis parameters with yields of [ $^{19}\text{F}$ ]FSK. ....	16
<b>Table 2.</b> Analytical HPLC examining radiochemical yields of [ $^{18}\text{F}$ ]FSK. ....	20

## LIST OF FIGURES

<b>Figure 1.</b> Chemoenzymatic Radiosynthesis/Synthesis of [ <sup>18/19</sup> F]FSK from [ <sup>18/19</sup> F]FDG. ....	10
<b>Figure 2.</b> <sup>1</sup> H NMR Spectra of Beta-D-glucose-1-phosphate. ....	14
<b>Figure 3.</b> <sup>19</sup> F-NMR Spectra of Chemoenzymatic Synthesis for trial 6. ....	17
<b>Figure 4.</b> Analytical HPLC for Radiosynthesis via Chemoenzymatic Process for [ <sup>18</sup> F]FSK, R1-R4. ....	19
<b>Figure 5.</b> Analytical HPLC for Radiosynthesis via Chemoenzymatic Process for [ <sup>18</sup> F]FSK. ....	21
<b>Figure 6.</b> <i>S. aureus</i> 1 (ATCC#12600) and 2 (ATCC#29213) Uptakes of improved [ <sup>18</sup> F]FSK. ....	22
<b>Figure 7.</b> <i>In vivo</i> Study conducted using [ <sup>18</sup> F]FSK. ....	23



## ABBREVIATIONS

2-deoxy-2-[<sup>18</sup>F]-fluoro-D-glucose ([<sup>18</sup>F]FDG)

2-deoxy-[<sup>18</sup>F]-fluoro-maltose ([<sup>18</sup>F]FDM)

2-deoxy-2-[<sup>18</sup>F]-fluoro-sakebiose ([<sup>18</sup>F]FSK)

Acetonitrile (MeCN)

American Type Culture Collection (ATCC#)

Beta-D-glucose-1-phosphate ( $\beta$ Glc-1P)

High Performance Liquid Chromatography (HPLC)

Maltose phosphorylase (MP)

Micro-positron emission tomography-computed tomography (microPET/CT)

Methicillin-resistant *S. aureus* (MRSA 01)

Nuclear Magnetic Resonance (NMR)

Radiochemical yield (RCY)

Room Temperature (R.T.)

*Staphylococcus aureus* (*S. aureus*)

*S. aureus* 1 (ATCC#12600) (SAA)

*S. aureus* 2 (ATCC#29213) (SAS)

Trifluoroacetic acid (TFA)

## SYMBOLS

Degree Celsius ( $^{\circ}\text{C}$ )

## Introduction

*Staphylococcus aureus*, commonly known as *S. aureus* or "staph," is a gram-positive bacterium that often colonizes the skin and gastrointestinal tract of humans without causing harm. However, when it enters the body through skin defects or other breaches, it can lead to severe infections such as pneumonia, osteomyelitis, and endocarditis.[1] People at higher risk of staph infections include children, infants, immunocompromised individuals, and those who have been hospitalized for extended periods.[2] These infections can range from minor skin conditions to life-threatening diseases, emphasizing the importance of proper hygiene and timely medical intervention to prevent and treat staph infections effectively.[3]

One radiotracer recently developed is 2-deoxy-2-[<sup>18</sup>F]-fluoro-sakebiose ([<sup>18</sup>F]FSK), which can be potentially accumulated by *S. aureus*. Glucose-based polysaccharides are responsive to enzymatic incorporation of unnatural monosaccharide units, opening the possibility of using the common clinical imaging tracer 2-deoxy-2-[<sup>18</sup>F]-fluoro-D-glucose ([<sup>18</sup>F]FDG) as a starting material to build complex glycans compatible with positron emission tomography (PET) imaging. A method is utilized to dimerize [<sup>18</sup>F]FDG, to form [<sup>18</sup>F]FSK for detecting microorganisms *in vivo* based on their bacteria-specific glycan incorporation. When [<sup>18</sup>F]FDG was reacted with beta-D-glucose-1-phosphate ( $\beta$ Glc-1P) in the presence of maltose phosphorylase (MP), both the alpha-1,4 and alpha-1,3-linked products 2-deoxy-[<sup>18</sup>F]-fluoro-maltose ([<sup>18</sup>F]FDM) and [<sup>18</sup>F]FSK were obtained.[4] With this method [<sup>18</sup>F]FDM is the main product, while [<sup>18</sup>F]FSK is the unanticipated product. Figure 1. illustrates the chemoenzymatic radiosynthesis/synthesis for [<sup>18/19</sup>F]FSK.

Based on Sorlin AM, et al.[4], it was shown that using nigerose phosphorylase (NP) instead of MP would yield only [<sup>18</sup>F]FSK, with a radiochemical yield (RCY) of 5%. However, it was also shown that when using MP the RCY for [<sup>18</sup>F]FSK was 15%. In this particular study the chemoenzymatic radiosynthesis for [<sup>18</sup>F]FSK was not optimized when using MP. It is valuable to improve the chemoenzymatic radiosynthesis for [<sup>18</sup>F]FSK using MP because NP is available only as a custom product and very expensive. We plan to refine the chemoenzymatic radiosynthesis to obtain [<sup>18</sup>F]FSK in a higher quantity since this disaccharide showed the best *in vitro* results. This work can offer an optimized chemoenzymatic radiosynthesis of the complex [<sup>18</sup>F]FDG-derived [<sup>18</sup>F]FSK to provide a future PET radiotracer for *S. aureus*.

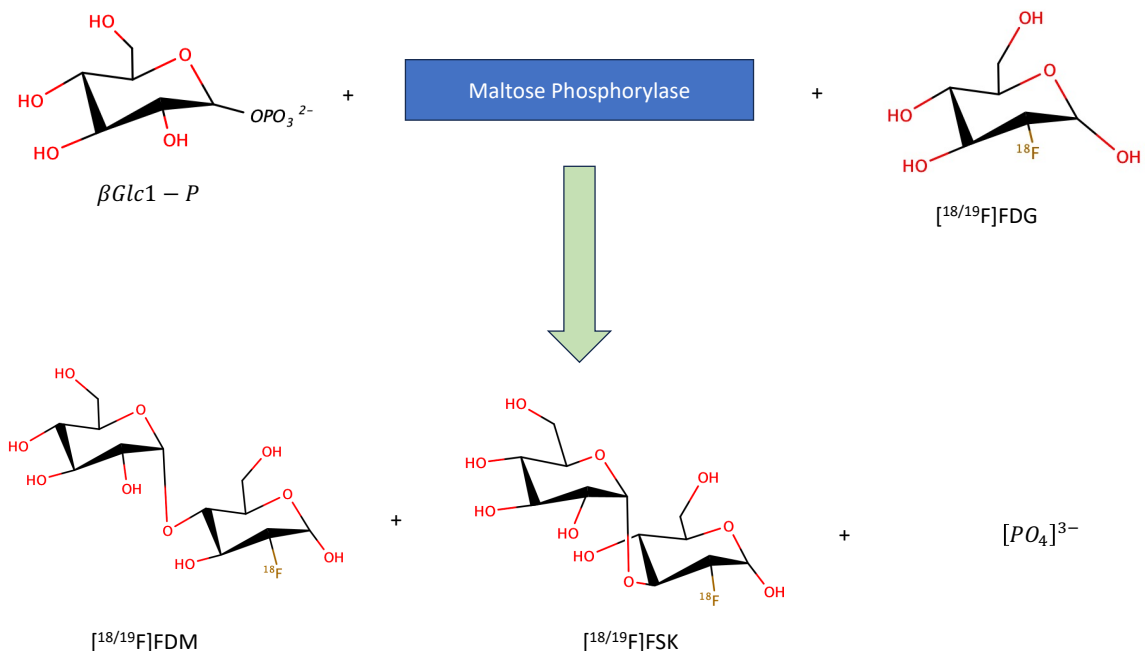


**Figure 1.** The notation of [ $^{18/19}$ F] is [ $^{19}$ F] or [ $^{18}$ F]. [ $^{18/19}$ F]FDG was reacted with  $\beta$ Glc-1P in the presence of maltose phosphorylase, both the alpha-1,4 and alpha-1,3-linked products [ $^{18/19}$ F]FDM and [ $^{18/19}$ F]FSK were obtained. All molecules were generated through MarvinSketch.

### Goals

- Optimize chemoenzymatic synthesis of [ $^{19}$ F]FSK.
- Apply new optimization to the [ $^{18}$ F]FSK radiosynthesis via chemoenzymatic process.
- Perform *in vitro* uptake evaluation of new [ $^{18}$ F]FSK in *S. aureus*.
- [ $^{18}$ F]FSK in  $\mu$ PET/CT on mice infected with *S. aureus*.<sup>[4]</sup>

### Methods

#### Materials

All chemical reagents were purchased from commercial sources (Acros Organics, Alfa Aesar, AK Scientific & Sigma-Aldrich) and used without further purification unless otherwise stated. The UCSF Radiopharmaceutical Facility provided the clinical sample of [ $^{18}$ F]FDG. All separatory cartridges were purchased from Waters. Reactions were monitored by thin layer chromatography (TLC) on precoated (250  $\mu$ m) silica gel 60 F254 aluminum sheets and visualized under a UV-254 lamp followed by staining with potassium permanganate. Flash chromatography was performed on silica gel (60A pore size).  $^1H$ , and  $^{19}F$  NMR spectra were obtained on a Bruker Avance III HD 400 MHz instrument at the UCSF Nuclear Magnetic

Resonance Laboratory and data were processed using MestReNova. Methicillin-resistant *S. aureus* (MRSA 01, MRSA Clinical isolate), was obtained from University of Nebraska Medical Center. The radioactivity of the bacterial pellets and filtrate were counted on a  $\gamma$  counter (Hidex Automatic Gamma Counter).

### **Preparation of beta-D-glucose-1-phosphate**

$\beta$ Glc-1P was synthesized in three steps from 1-bromo- $\alpha$ -D-glucose tetraacetate. The synthesis of  $\beta$ Glc-1P was conducted according to the supporting information from Sorlin AM, et al.[4].

### **[ $^{19}\text{F}$ ]FSK Synthesis**

Beta-D-glucose-1-phosphate ( $\beta$ Glc-1P) (9.0 mg, 0.03 mmol – 54.1 mg, 0.17 mmol), 2-deoxy-2[ $^{19}\text{F}$ ]-fluoroglucose (4.2mg, 0.02 mmol – 12.5 mg, 0.07mmol) were added to a 10 mL round bottom flask containing maltose phosphorylase (EC 2.4.1.8, Sigma Aldrich), (0.4 mg, 4 units - 3.5 mg, 35 units) in 3 mL of aqueous citrate buffer solution (pH = 6.5). The mixture was stirred between 20 min. to 3 days 6 hours at temperatures 25 °C to 50 °C. The mixture was prepared for NMR analysis, for quantification of [ $^{19}\text{F}$ ]FSK.

### **[ $^{19}\text{F}$ ]FSK NMR Preparation**

The reaction was treated with 2  $\mu\text{L}$  of trifluoroacetic acid (TFA). TFA is used as a standard for  $^{19}\text{F}$  identification in NMR analysis. Deuterium oxide ( $\text{D}_2\text{O}$ , 0.5 mL) was added as a solvent into the mixture contained in the vial. Followed by the addition of 0.3 mL MeCN was added into the vial in order to terminate the activity of maltose phosphorylase. The mixture was analyzed with NMR (Bruker Avance III HD 400).

### **[ $^{18}\text{F}$ ]FSK Synthesis**

In a 4 mL borosilicate vial containing PTFE stir bar, maltose phosphorylase (EC 2.4.1.8, Sigma Aldrich), (0.3 mg, 3 units - 0.9mg, 9 units) and  $\beta$ Glc1-P (1.5 mg, 0.01mmol – 9.0 mg, 0.03 mmol) were added. A dose of clinical [ $^{18}\text{F}$ ]FDG (10-15 mCi) in citrate buffer (0.1M, pH=6.0, 0.15-0.3 mL) was directly transferred to the vial and the mixture was stirred at 37 °C for 20 min to 60 min. Quantification for [ $^{18}\text{F}$ ]FSK was done through analytical HPLC, while semi-prep HPLC was used for *in vitro* or *in vivo* studies.

### *Analytical HPLC*

The reaction (10  $\mu$ L) was diluted with 0.1 mL of the mobile phase, consisting of 77% MeCN 23% H<sub>2</sub>O to match the HPLC column (YMC-Pack Polyamine II, 250X10 nm). The stationary phase was YMC-Pack Polyamine II column and the mobile phase of 77:23 acetonitrile/H<sub>2</sub>O at a flowrate of 1 mL/min. Inject 10  $\mu$ L of sample into HPLC.

### *Semi-Prep HPLC*

The reaction was diluted with MeCN then filtered through C18 light cartridge, before being purified via semi prep HPLC (YMC-Pack Polyamine II, 250 X 10 mm). For semi-prep HPLC, a YMC-Pack Polyamine II stationary phase was used with a mobile phase of 73:27 acetonitrile/H<sub>2</sub>O at a flowrate of 4 mL/min..

[<sup>18</sup>F]FSK was isolated in 5-7mL fractions. The fractions were then diluted with MeCN (40 mL) before being passed through Sep-pak Plus NH<sub>2</sub> Cartridge at 5 mL/min to trap each dimer product. After flushing the cartridge with air and N<sub>2</sub> gas, they were eluted using saline solution for direct formulation before use *in vitro* or *in vivo*.

### ***In vitro* Uptake Evaluation in *Staphylococcus aureus***

*S. aureus*, was grown overnight in lysogeny broth (LB) in a shaking incubator at 37 °C. An overnight culture was diluted to an optical density at 600 nm (OD<sub>600</sub>) of 0.05 and grown to exponential phase (~ 0.4- 0.6). The bacterial culture was incubated with 24  $\mu$ Ci of [<sup>18</sup>F]FSK at 37 °C for 90 minutes for uptake study. After tracer incubation, 500  $\mu$ L of the bacterial culture was transferred to Spin-X LC 1.5 mL tubes (0.22  $\mu$ m) and was centrifuged (6 min, 13200 rpm) to separate bacterial cells and supernatant. Bacterial cells were then washed 1x with phosphate buffered saline (PBS) to remove any tracer not taken up by bacteria. Heat-killed bacterial sample used as control was prepared by incubating the bacterial culture at 90 °C for 30 min. Retained radiotracer within sample was then counted using an automated gamma-counter (Hidex).

## **μPET/CT imaging**

All animal procedures were approved by the UCSF Institutional Animal Care and Use Committee and were performed in accordance with UCSF guidelines.

### *In vivo [<sup>18</sup>F]FSK dynamic μPET/CT imaging in a myositis mouse model*

The bacteria culture was prepared as stated in the *in vitro* uptake evaluation in *S. aureus* method. Mice were inoculated with *S. aureus* in the left deltoid muscle and ten-fold higher bacterial load of heat killed bacteria in the right deltoid muscle. Twelve hours after inoculation, [<sup>18</sup>F]FSK was injected via tail vein (~100 μL, 200 μCi, containing 1 mg voglibose). The mice were imaged by μPET/CT (Inveon μPET-CT) using 90-minute dynamic PET scan with a five-minute CT. PET data was analyzed using the open-source AMIDE software. Uptake quantification was performed by drawing spherical regions of interest (5-8 mm<sup>3</sup>) over the specified organs on the CT and expressed as the percentage of the injected dose per gram. [4] For the synthesis, the RCY was decay-corrected for [<sup>18</sup>F] ( $t_{1/2}$ =109.7 minutes [5]). The statistical analyses were conducted using GraphPad Prism version 9. An unpaired two-tailed Student's t-test was applied for data analysis. Error bars in all graphs represent the standard error of the mean.[4]

## **Results**

### **Beta-D-glucose-1-phosphate**

Figure 2. provides a <sup>1</sup>H NMR spectra of βGlc-1P. The spectra was obtained in order to justify the use of the synthesized βGlc-1P in production of [<sup>18/19</sup>F]FSK. It was compared to the spectroscopic data provided by Sorlin AM, et al.[4].

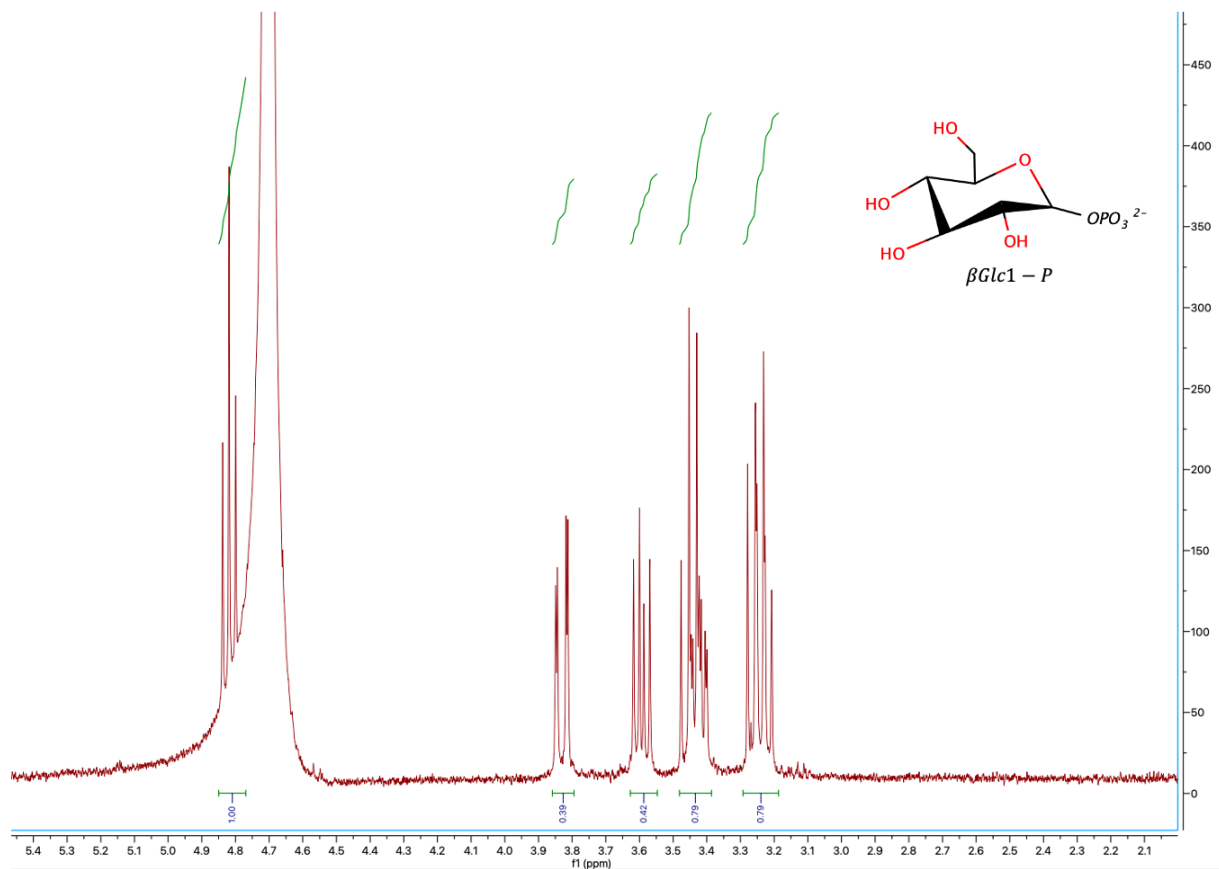


**Figure 2.**  $^1\text{H}$  NMR spectra of beta-D-glucose-1-phosphate. Spectra analyzed through MestReNova.

### $^{19}\text{F}$ FSK Trials

$^{19}\text{F}$ FDG reacts with  $\beta\text{Glc-1P}$  in the presence of maltose phosphorylase (MP), yielding both the alpha-1,4 and alpha-1,3-linked products  $^{19}\text{F}$ FDM and  $^{19}\text{F}$ FSK as shown in Figure 1. To assess the masses of these products from different reactions, NMR analysis was performed. Quantitative NMR was computed for each reaction by using the integration provided from MestReNova. TFA was used as a standard in order to calculate the mass of each compound given the integration. Table 1. provides the total mass for all products formed in reactions and denotes the parameters that were changed. The control experiment (Trial 1) used 0.9 mg maltose phosphorylase (MP), 18.1 mg  $\beta\text{Glc-1P}$ , 12.5 mg  $^{19}\text{F}$ FDG, 0.5 mL citrate buffer, at a temperature of  $37^\circ\text{C}$ , and was stirred for 20 minutes. The total mass ratio between  $^{19}\text{F}$ FSK and  $^{19}\text{F}$ FDM was 1.08mg : 5.40mg. Based on the control experiment, one of the parameters was altered while keeping the others constant. Trials 2 and 3 investigated temperature variations. The temperatures used were  $25^\circ\text{C}$  and  $50^\circ\text{C}$ . Both trials did not show any production of  $^{19}\text{F}$ FSK and  $^{19}\text{F}$ FDM. Trials 4 through 6 examined different amounts of MP, using between 0.3 mg - 3.5 mg. Trial 4 decreased MP to 0.4 mg, the total mass



ratio was 0.54 mg [<sup>19</sup>F]FSK : 5.94 mg [<sup>19</sup>F]FDM. Trial 5 increased MP to 1.8 mg, the total mass ratio was 2.70 mg [<sup>19</sup>F]FSK : 4.86 mg [<sup>19</sup>F]FDM. Trial 6 increased MP to 3.5 mg, the total mass ratio was 4.32 mg [<sup>19</sup>F]FSK : 3.24 mg [<sup>19</sup>F]FDM. An [<sup>19</sup>F]-NMR spectrum in Figure 3. shows the integrations for [<sup>19</sup>F]FSK, [<sup>19</sup>F]FDM, and [<sup>19</sup>F]FDG in trial 6, with integrations of 0.16 for [<sup>19</sup>F]FSK, 0.12 for [<sup>19</sup>F]FDM, and 0.29 for [<sup>19</sup>F]FDG. Subsequently, Trials 7 through 9 tested varying amounts of βGlc-1P ranging from 9.0 mg and 54.1 mg. Trial 7 decreased the βGlc-1P to 9.0 mg, the total mass ratio was 1.08 mg [<sup>19</sup>F]FSK : 1.89 mg [<sup>19</sup>F]FDM. Trial 8 increased the βGlc-1P to 35.9 mg, the total mass ratio was 0.81 mg [<sup>19</sup>F]FSK : 14.57 mg [<sup>19</sup>F]FDM. Trial 9 increased the βGlc-1P to 54.1 mg, the total mass ratio was 0.54 mg [<sup>19</sup>F]FSK : 13.76 mg [<sup>19</sup>F]FDM. Finally, trials 10 through 12 tested various reaction times, spanning from 18 hours-10 minutes and 3 days-360 minutes. Trial 10 increased the time by 1,070 minutes, resulting in a total mass ratio 2.15 mg [<sup>19</sup>F]FSK : 0.54 mg [<sup>19</sup>F]FDM. Trial 11 increased the time by 1,420 minutes, the total mass ratio was 1.89 mg [<sup>19</sup>F]FSK : 0.54 mg [<sup>19</sup>F]FDM. Trial 12 increased the time by 4,680 minutes, the total mass ratio was 1.08 mg [<sup>19</sup>F]FSK : 0.27 mg [<sup>19</sup>F]FDM.

**Table 1.** [<sup>19</sup>F]FSK chemoenzymatic synthesis parameter with total mass amounts produced of [<sup>19</sup>F]FSK. Results from parameters changes in the chemoenzymatic synthesis of [<sup>19</sup>F]FSK including the production mass of [<sup>19</sup>F]FSK (mg), [<sup>19</sup>F]FDM (mg), and [<sup>19</sup>F]FDG (mg). Trial 1 is the control based on Sorlin AM, et al.[4].

Trials	Changing Variable	TEMP (°C)	Maltose Phosphorylase	<i>βGlc1-P</i>	TIME	FDG	Yield [ <sup>19</sup> F]FSK (mg)	Yield [ <sup>19</sup> F]FDM (mg)	By-Product FDG (mg)
1	Temp	37	0.9 mg	18.1 mg	20 min	12.5 mg	1.08	5.40	4.14
2	Temp	25	0.9 mg	18.1mg	20 min	12.5 mg	0.00	0.00	6.99
3	Temp	50	0.9 mg	18.1mg	20 min	12.5 mg	0.00	0.00	12.1
4	Enzyme	37	0.4 mg	18.1 mg	20 min	12.5 mg	0.54	5.94	4.14
5	Enzyme	37	1.8 mg	18.1 mg	20 min	12.5 mg	2.70	4.86	4.14
6	Enzyme	37	3.5 mg	18.0 mg	20 min	12.6 mg	4.32	3.24	4.14
7	<i>βGlc1-P</i>	38	0.8 mg	9.0 mg	21 min	12.5 mg	1.08	1.89	5.14
8	<i>βGlc1-P</i>	38	0.8 mg	35.9 mg	21 min	12.5 mg	0.81	14.57	3.28
9	<i>βGlc1-P</i>	38	0.9 mg	54.1 mg	21 min	12.5 mg	0.54	13.76	1.57
10	Time	37	0.5 mg	6.7 mg	18 hr 10 min	4.2 mg	2.15	0.54	1.29
11	Time	37	0.5 mg	6.7 mg	24 hr	4.3 mg	1.89	0.54	1.29
12	Time	37	0.5 mg	6.7 mg	3 days 6 hr	4.2 mg	1.08	0.27	1.29

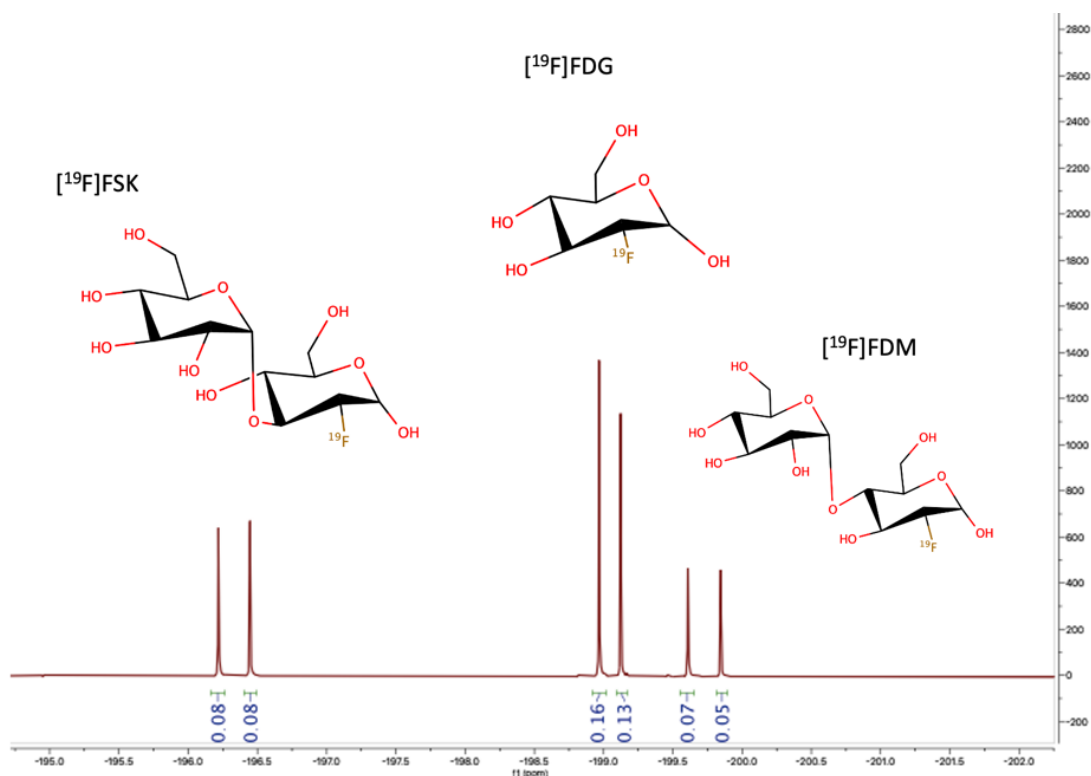


**Figure 3.**  $^{19}\text{F}$ -NMR spectra of chemoenzymatic synthesis for trial 6. With  $^{19}\text{F}$ ]FSK integration of 0.16,  $^{19}\text{F}$ ]FDM integration of 0.12, and  $^{19}\text{F}$ ]FDG integration of 0.29. Spectra generated through MestReNova and molecules drawn through MarvinSketch.

### $^{18}\text{F}$ ]FSK Trials

$^{18}\text{F}$ ]FDG reacts with  $\beta\text{Glc-1P}$  in the presence of MP, yielding both the alpha-1,4 and alpha-1,3-linked products  $^{18}\text{F}$ ]FDM and  $^{18}\text{F}$ ]FSK as indicated in Figure 1. Analytical HPLC was used to evaluate the radiochemical yield percentage of these products, from different reactions. The control experiment (Trial R1) used 0.3 mg maltose phosphorylase, 6 mg  $\beta\text{Glc-1P}$ , 0.3 mL  $^{18}\text{F}$ ]FDG, at a temperature of  $37^\circ\text{C}$ , and was stirred for 20 minutes. The radiochemical yield percentage for  $^{18}\text{F}$ ]FSK was 4.64%. Based on the control experiment, one or more parameters were changed while keeping the rest constant. Table 2. provides the radiochemical yield percentage (RCY %) for all reactions performed and denotes the parameters that were changed. Trials R2 through R4 investigated time variations, with times of 30, 40, and 60 minutes. The resulting RCY% for  $^{18}\text{F}$ ]FSK were 7.08%, 8.81%, and 7.26%. Figure 4. illustrates the analytical HPLC runs for Trials R1 through R4. The first peak represents  $^{18}\text{F}$ ]FDG, the second represents  $^{18}\text{F}$ ]FDM, and the last represents  $^{18}\text{F}$ ]FSK.  $^{18}\text{F}$ ]FDG peaks between 15-20 minutes,  $^{18}\text{F}$ ]FDM between 20-45 minutes, and  $^{18}\text{F}$ ]FSK at 22, 30, or 65 minutes, depending on the mobile phase used. Trials R5

through R7 investigated variations in enzyme and precursor amounts. The enzyme concentration was doubled compared to the control experiment in these trials. The precursor amount was decreased in Trials R5 and R6 and increased in Trial R7. The resulting RCY% for [<sup>18</sup>F]FSK were 38.9%, 54.12%, and 48.56%. Trials R8 through R10 investigated variations in enzyme, precursor, and clinical [<sup>18</sup>F]FDG amounts. The enzyme was doubled or tripled compared to the control experiment in these trials, and the precursor amount was decreased. The resulting RCY% for [<sup>18</sup>F]FSK were 35.7%, 37.44%, and 42.93%. Figure 5. presents the analytical HPLC runs for Trials R5 through R10. The first peak represents [<sup>18</sup>F]FDG, the second represents [<sup>18</sup>F]FDM, and the last represents [<sup>18</sup>F]FSK. [<sup>18</sup>F]FDG peaks around the 16th minute, [<sup>18</sup>F]FDM around the 23rd minute, and [<sup>18</sup>F]FSK around the 30th minute using a mobile phase of 77% MeCN and 23% H<sub>2</sub>O. The average RCY for [<sup>18</sup>F]FSK in Trials R5 through R10 was calculated to be 42.94% ± 6.53% standard deviation (SD).

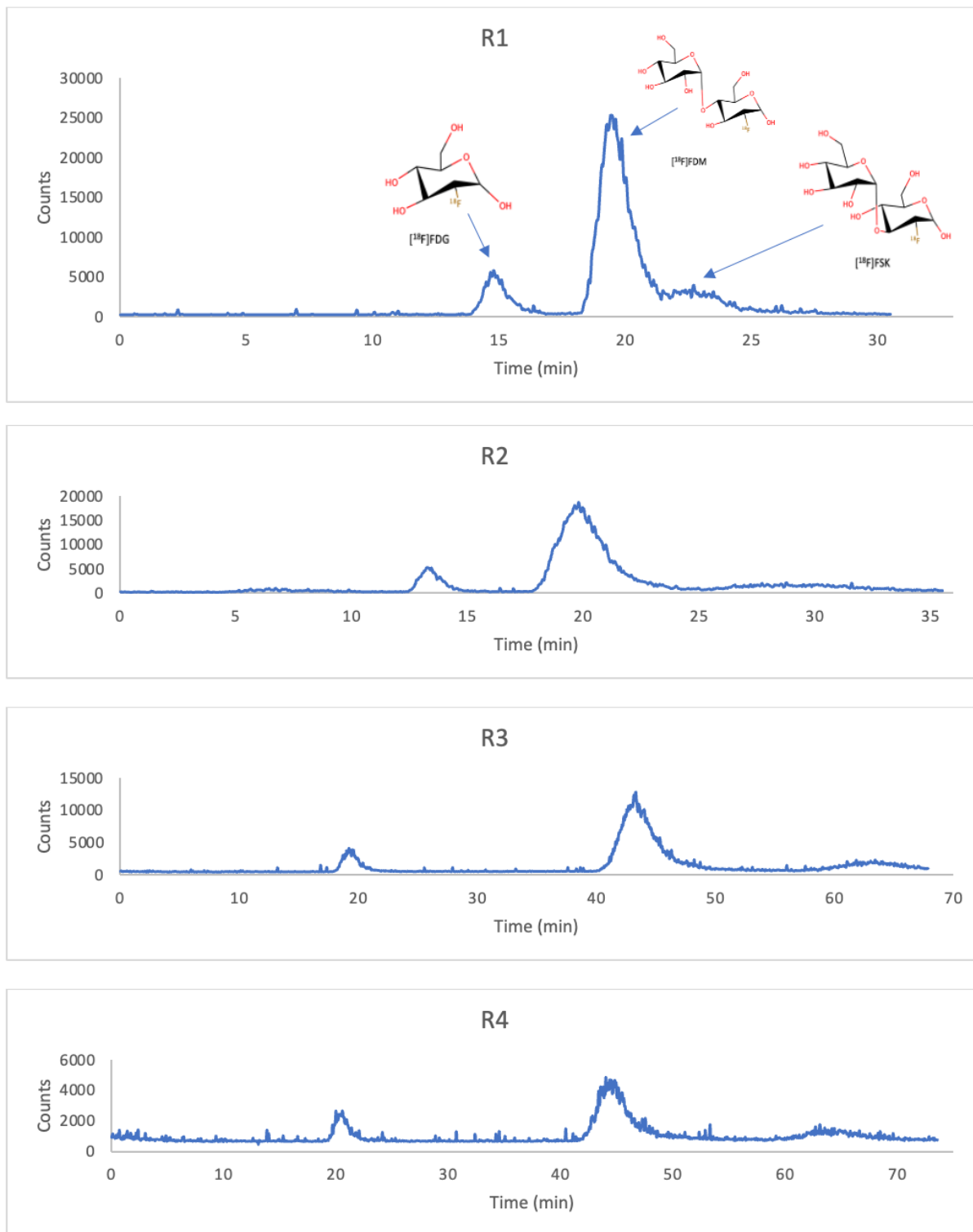


**Figure 4.** Analytical HPLC for radiosynthesis via chemoenzymatic process for  $[^{18}\text{F}]\text{FDSK}$ . Inclusion of trials R1 through R4.

**Table 2.** Analytical HPLC Examining Radiochemical Yield of [<sup>18</sup>F]FSK.

Trials	Changing Variable	TEMP (°C)	Enzyme (mg)	Precursor (mg)	Time (min)	Clinical [ <sup>18</sup> F]FDG (mL)	Mobile Phase	RCY% FDG	RCY% FDM	RCY% FSK
R1	Time	37	0.3	6	20	0.3	73% MeCN	12.54	77.99	4.64
R2	Time	37	0.3	6	30	0.2	85% MeCN	9.61	76.29	7.08
R3	Time	37	0.3	6	40	0.2	85% MeCN	8.90	65.02	8.81
R4	Time	37	0.3	6	60	0.2	85% MeCN	8.38	40.94	7.26
R5	MP + $\beta$ Glc-1P	37	0.6	1.5	20	0.2	77% MeCN	36.83	24.25	38.90
<b>R6</b>	MP + $\beta$ Glc-1P	37	0.5	3	20	0.2	77% MeCN	12.31	32.14	54.12
<b>R7</b>	MP + $\beta$ Glc-1P	37	0.6	9	20	0.2	77% MeCN	16.48	34.39	48.56
R8	MP + $\beta$ Glc-1P	37	0.6	1.5	20	0.2	77% MeCN	18.48	37.49	35.70
R9	MP + $\beta$ Glc-1P	37	0.6	3	20	0.2	77% MeCN	15.48	40.28	37.44
<b>R10</b>	MP + $\beta$ Glc-1P + [ <sup>18</sup> F]FDG	37	0.9	3	20	0.15	77% MeCN	32.46	13.98	42.93

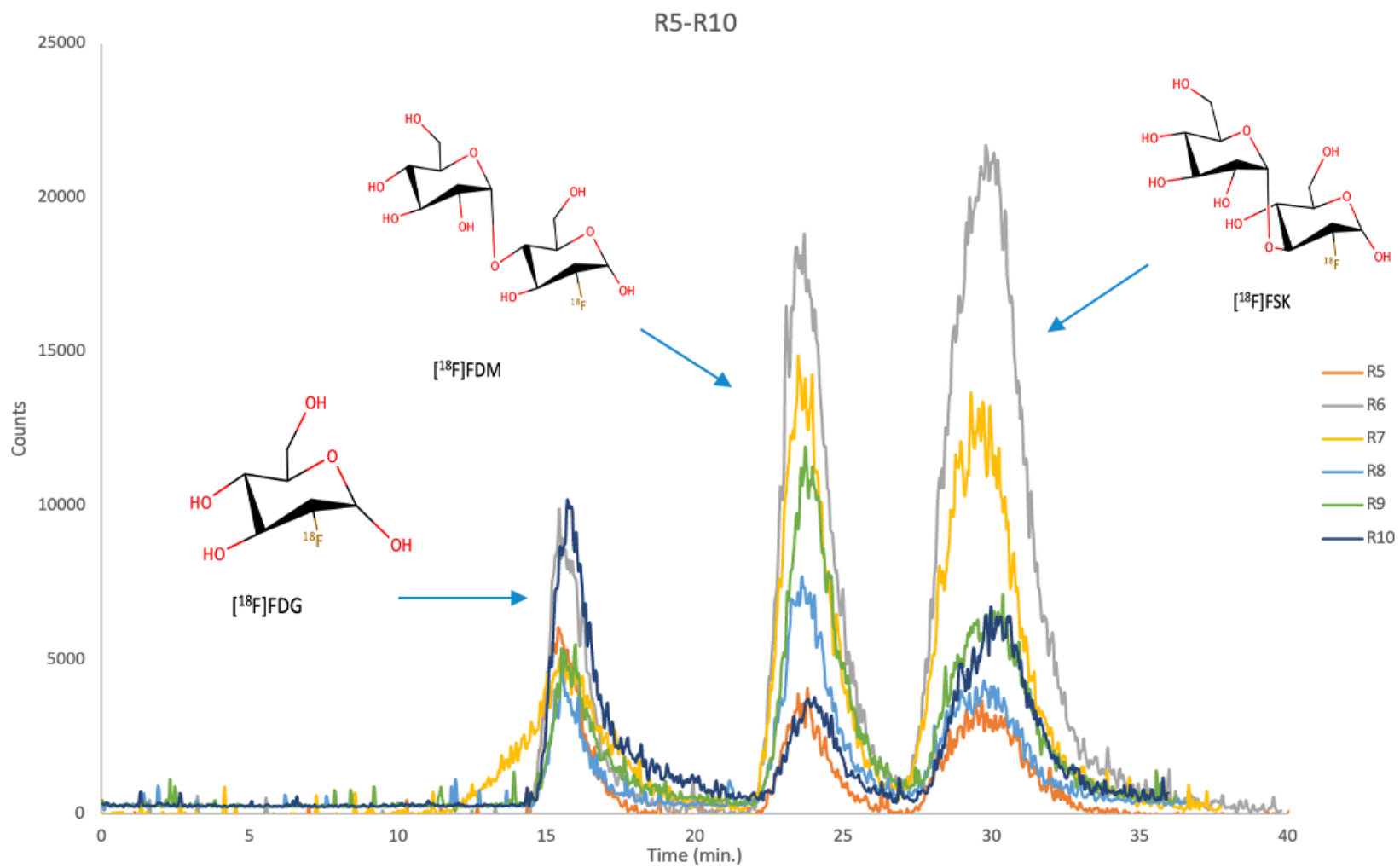


**Figure 5.** Analytical HPLC for radiosynthesis via chemoenzymatic process for  $[^{18}\text{F}]$ FSK. Inclusion of trials R5 through R10.

### **[<sup>18</sup>F]FSK *In vitro* Uptake Evaluation in *Staphylococcus aureus***

The examination of the improved tracer [<sup>18</sup>F]FSK *in vitro* aimed to evaluate its incorporation into two different strains of *S. aureus*. As shown in Figure 6., [<sup>18</sup>F]FSK was incorporated into *S. aureus* strains 1 and 2. For *S. aureus* strain 1, the cellular uptake was approximately 24 Bq per 10<sup>6</sup> cells, while for *S. aureus* strain 2, it was approximately 17 Bq per 10<sup>6</sup> cells.

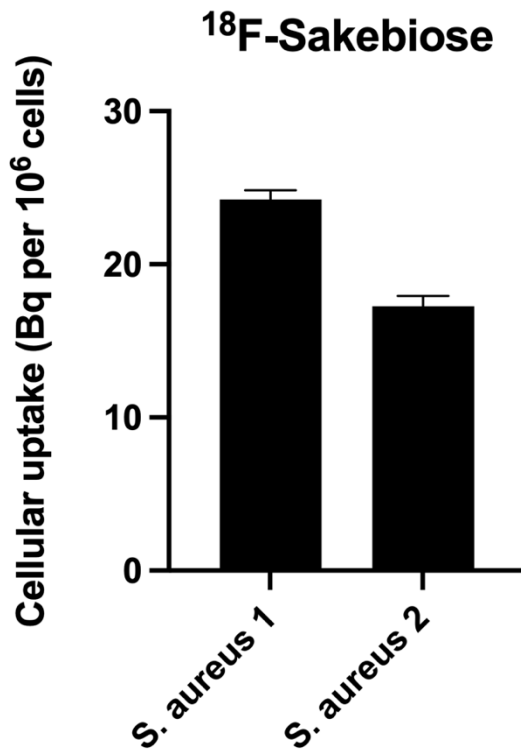


**Figure 6.** *S. aureus* 1 (ATCC#12600) and 2 (ATCC#29213) uptakes of improved [<sup>18</sup>F]FSK. The error bars represent the standard error of mean (SEM).

### **[<sup>18</sup>F]FSK *In Vivo* Dynamic Imaging**

The evaluation of [<sup>18</sup>F]FSK uptake in MRSA 01 infection was conducted using a mouse myositis model, as demonstrated in Figure 7. Mice were inoculated with MRSA 01 in the left deltoid muscle and a ten-fold higher bacterial load of heat-killed bacteria in the right deltoid muscle.[4] The inhibitor used was voglibose at a rate of 1 mg/injection. The injection contained approximately 200  $\mu$ Ci of [<sup>18</sup>F]FSK, N=6.[4] Red arrows indicate the site of inoculation with live bacteria, while white arrows indicate the site of inoculation with heat-killed bacteria. The *ex vivo* data was obtained following tissue harvesting and gamma counting. The *in vivo*



region of interest (ROI) analysis between heat-killed versus live bacteria showed a 6.5-fold increase, with a \*\*\*\*  $P$  value  $< 0.0001$ . [4] Additionally, the *ex vivo* analysis between live and heat-killed bacteria showed a 4.7-fold increase, with a \*\*\*\*  $P$  value  $< 0.0001$  (unpaired t-test). [4]

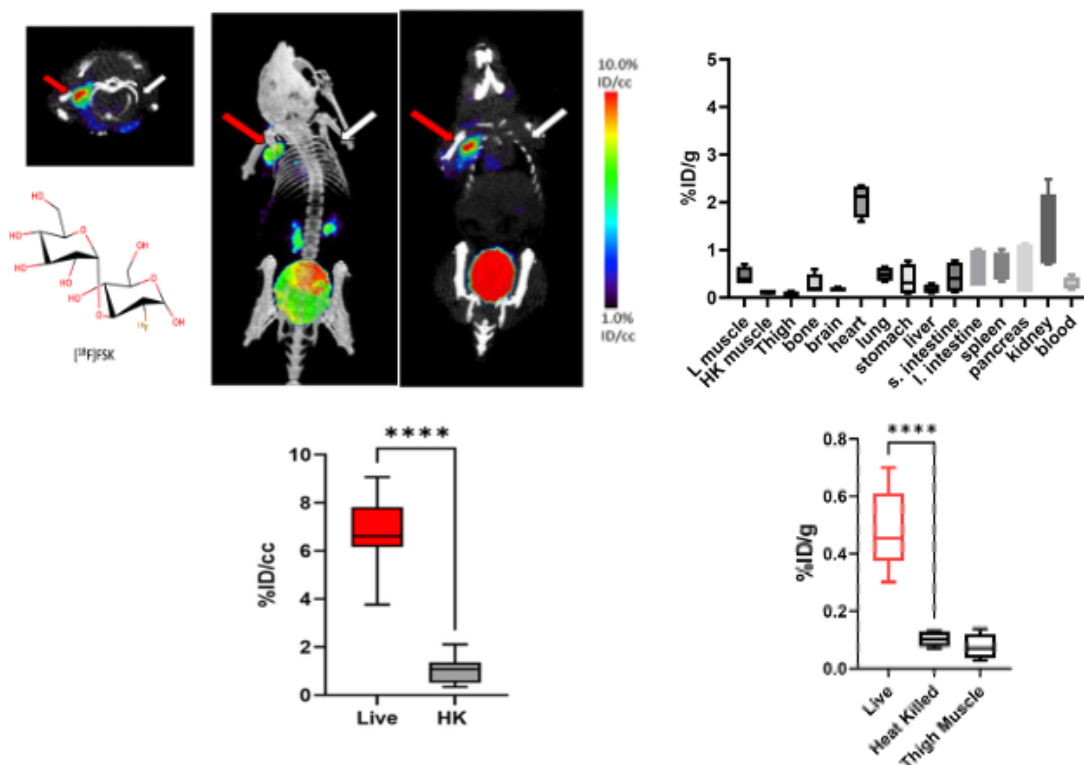


**Figure 7.** An *in vivo* study was conducted using [ $^{18}\text{F}$ ]FSK in a mouse myositis model which was induced by methicillin-resistant *S. aureus* (MRSA 01). (All rights reserved to Sorlin AM, López-Álvarez M, Rabbitt SJ, Alanizi AA, Shuere R, Bobba KN, Blecha J, Sakhamuri S, Evans MJ, Bayles KW, Flavell RR, Rosenberg OS, Sriram R, Desmet T, Nidetzky B, Engel J, Ohliger MA, Fraser JS, Wilson DM. Chemoenzymatic Syntheses of Fluorine-18-Labeled Disaccharides from [ $^{18}\text{F}$ ] FDG Yield Potent Sensors of Living Bacteria *In Vivo*. *J Am Chem Soc.* 2023 Aug 16;145(32):17632-17642. doi: 10.1021/jacs.3c03338. Epub 2023 Aug 3. PMID: 37535945; PMCID: PMC10436271.)

## Discussion

The chemoenzymatic synthesis for [ $^{19}\text{F}$ ]FSK was optimized to gain insight into the parameters that should be adjusted to optimize the chemoenzymatic radiosynthesis of [ $^{18}\text{F}$ ]FSK. Trials 6, 7, 10, 11, and 12 showed the best total mass ratio for producing [ $^{19}\text{F}$ ]FSK. Trial 6 used approximately a four-fold increase in maltose phosphorylase, resulting in a total mass of 4.32 mg of [ $^{19}\text{F}$ ]FSK compared to 3.24 mg of [ $^{19}\text{F}$ ]FDM. Trial 10 extended the reaction time by 1,070 min., leading to a total mass of 2.15 mg of [ $^{19}\text{F}$ ]FSK compared to 0.54

mg of [<sup>19</sup>F]FDM. Trials 2- 5, 8 and 9 did not produce significant total masses of [<sup>19</sup>F]FSK; however, their results were used in the chemoenzymatic radiosynthesis for [<sup>18</sup>F]FSK.

For the chemoenzymatic radiosynthesis of [<sup>18</sup>F]FSK, the most promising parameters were derived from the [<sup>19</sup>F]FSK synthesis. The key factors that improved [<sup>18</sup>F]FSK production, by increasing the yield from an initial radiochemical yield (RCY) of 5% in the control experiment, was higher MP concentration and lower βGlc-1P amounts. Additionally, trial R10, despite a decrease in [<sup>18</sup>F]FDG, still achieved a RCY% higher than the control. Trials R5 through R10 resulted in [<sup>18</sup>F]FSK RCYs greater than 35%, with an average RCY of 42.94% ± 6.53% (SD). These findings suggest that increasing MP concentration and decreasing βGlc-1P amount significantly enhanced the production of [<sup>18</sup>F]FSK, increasing the RCY by about 30%.

*S. aureus* can lead to severe infections such as pneumonia, osteomyelitis, and endocarditis once a viable infection is established. The improved tracer ([<sup>18</sup>F]FSK) was evaluated *in vitro* for its incorporation into two different strains of *S. aureus*. Cellular uptake of [<sup>18</sup>F]FSK was significant in both strains, as shown in Figure 6. In evaluating [<sup>18</sup>F]FSK uptake in MRSA 01 infection using a mouse myositis model, ROI analysis revealed that [<sup>18</sup>F]FSK uptake at the site of live MRSA 01 injection was 6.5 times higher than at the site of heat-killed MRSA injection.[4] Additionally, *ex vivo* analysis through tissue harvesting and gamma counting further validated the results, showing that the mean [<sup>18</sup>F]FSK accumulation in tissues inoculated with live MRSA 01 was 4.7 times higher than in tissues inoculated with heat-killed bacteria (*P* value < 0.0001 for [<sup>18</sup>F]FSK).[4]

Notably, the optimized chemoenzymatic radiosynthesis of [<sup>18</sup>F]FSK using MP, will be a promising route for developing the tracer to be used in detection and monitoring of *S. aureus* infections using PET/CT imaging. The refined synthesis using MP demonstrated a 30% RCY or greater for [<sup>18</sup>F]FSK. Additionally, MP is commercially available and more cost-effective compared to NP. Complete optimization could be further explored for the chemoenzymatic radiosynthesis of [<sup>18</sup>F]FSK using higher concentrations of MP or varying temperatures.

## Conclusion

This study effectively optimized the chemoenzymatic synthesis of [ $^{19}\text{F}$ ]FSK, demonstrating significant improvements in yield by adjusting key parameters such as MP concentration,  $\beta\text{Glc-1P}$  levels, and reaction time. The optimized conditions were then applied to the radiosynthesis of [ $^{18}\text{F}$ ]FSK, resulting in a 30% increase in radiochemical yield as determined by analytical HPLC. *In vitro* experiment confirmed that [ $^{18}\text{F}$ ]FSK is readily incorporated into two strains of *Staphylococcus aureus*, highlighting its potential as a PET radiotracer for bacterial infections. Furthermore, preliminary *in vivo* imaging study in a mouse model showed promising uptake of [ $^{18}\text{F}$ ]FSK in infected tissues. These findings hint at a new route for [ $^{18}\text{F}$ ]FSK to be a valuable tool for the non-invasive detection and monitoring of *S. aureus* infections using PET/CT imaging.

## References

- [1] "Staphylococcus Aureus Basics." *Centers for Disease Control and Prevention*, Centers for Disease Control and Prevention, [www.cdc.gov/staphylococcus-aureus/about/index.html](http://www.cdc.gov/staphylococcus-aureus/about/index.html). Accessed 8 July 2024.
- [2] "Staphylococcus Aureus Infections - Staphylococcus Aureus Infections." *Merck Manual Consumer Version*, [www.merckmanuals.com/home/infections/bacterial-infections-gram-positive-bacteria/staphylococcus-aureus-infections](http://www.merckmanuals.com/home/infections/bacterial-infections-gram-positive-bacteria/staphylococcus-aureus-infections). Accessed 8 July 2024.
- [3] "Staph Infections." *Mayo Clinic*, Mayo Foundation for Medical Education and Research, [www.mayoclinic.org/diseases-conditions/staph-infections/symptoms-causes/syc-20356221](http://www.mayoclinic.org/diseases-conditions/staph-infections/symptoms-causes/syc-20356221). Accessed 8 July 2024.
- [4] Sorlin AM, López-Álvarez M, Rabbitt SJ, Alanizi AA, Shuere R, Bobba KN, Blecha J, Sakhamuri S, Evans MJ, Bayles KW, Flavell RR, Rosenberg OS, Sriram R, Desmet T, Nidetzky B, Engel J, Ohliger MA, Fraser JS, Wilson DM. Chemoenzymatic Syntheses of Fluorine-18-Labeled Disaccharides from [<sup>18</sup>F] FDG Yield Potent Sensors of Living Bacteria *In Vivo*. *J Am Chem Soc*. 2023 Aug 16;145(32):17632-17642. doi: 10.1021/jacs.3c03338. Epub 2023 Aug 3. PMID: 37535945; PMCID: PMC10436271.
- [5] Henry F. VanBrocklin, Chapter 25 - PET Radiochemistry, Editor(s): Brian D. Ross, Sanjiv Sam Gambhir, *Molecular Imaging (Second Edition)*, Academic Press, 2021, Pages 445-478, ISBN 9780128163863, <https://doi.org/10.1016/B978-0-12-816386-3.00027-2>.

## Publishing Agreement

It is the policy of the University to encourage open access and broad distribution of all theses, dissertations, and manuscripts. The Graduate Division will facilitate the distribution of UCSF theses, dissertations, and manuscripts to the UCSF Library for open access and distribution. UCSF will make such theses, dissertations, and manuscripts accessible to the public and will take reasonable steps to preserve these works in perpetuity.

I hereby grant the non-exclusive, perpetual right to The Regents of the University of California to reproduce, publicly display, distribute, preserve, and publish copies of my thesis, dissertation, or manuscript in any form or media, now existing or later derived, including access online for teaching, research, and public service purposes.

Signed by:

*Nadezhda A. Urmanov*

43EF62C7E60D482...

Author Signature

8/29/2024

Date